Dalton Transactions

Synthesis of disubstituted furans catalysed by [$(AuCl)_2$(μ-bis(phosphino)metallocene)] and Na[$BArF_{24}$]

Journal:	*Dalton Transactions*
Manuscript ID	DT-ART-09-2022-002999.R1
Article Type:	Paper
Date Submitted by the Author:	18-Oct-2022
Complete List of Authors:	Gwinn, Reilly; Lafayette College, Chemistry Boggess, Anna; Lafayette College, Chemistry Winter, Elizabeth; Lafayette College, Chemistry Nataro, Chip; Lafayette College, Chemistry

ARTICLE

Synthesis of disubstituted furans catalysed by [(AuCl)$_2$(μ-bis(phosphino)metallocene)] and Na[BArF$_{24}$]

Received 00th January 20xx,
Accepted 00th January 20xx

DOI: 10.1039/x0xx00000x

Reilly K. Gwinn,‡ Anna E. Boggess, Elizabeth P. Winter and Chip Nataro*

The catalytic activity of a series of [(AuCl)$_2$(μ-PP)] (PP = 1,1'-bis(phosphino)metallocene ligands) compounds in the presence of Na{BArF$_{24}$] (BArF$_{24}$ = tetrakis(3,5-bis(trifluoromethyl)phenyl borate) was examined in the formation of disubstituted furans from pyridine-*N*-oxide and terminal alkynes. The products of these reactions were typically the 2,5-disubstituted furans, but in the case of using 2-ethynylpyridene, the 2,4-disubstituted furan formed. The catalytic efficiency was dependent upon both the nature of the terminal alkyne and the 1,1'-bis(phosphino)metallocene ligands. During the course of this study, two new compounds, [(AuCl)$_2$(μ-dppr)] and [(AuCl)$_2$(μ-dppo)] (dppr = 1,1'-bis(diphenylphosphino)ruthenocene; dppo = 1,1'-bis(diphenylphosphino)osmocene), were prepared and characterized by NMR. X-ray crystal structures of both compounds were determined and the oxidative electrochemistry of these new compounds was examined.

Introduction

Furans have been identified in many naturally occurring bioactive molecules[1–7] derived from cooking oils,[8–11] plants,[10–13] and marine life.[14] With the variety of naturally occurring furans, this functionality has been utilized by the pharmaceutical and agrochemical industries in many different commercially available products.[1–7] While some furans are carcinogenic,[15] many show promising activity as antifungal agents, antiviral agents, antitumor agents, and analgesics.[1–7,16,17] The difference in the activity of these compounds is associated with the complex substitution on and incorporation of the furan ring, especially in the context of structure-activity relationships for medication. For example, the Human Immunodeficiency Virus (HIV) medication darunavir and the antibiotic nitrofurantoin both incorporate furan rings that are distinct in substitution pattern and group, as well as carbon saturation (Fig. 1).[16,17] Based on the structure and applications of these and other bioactive furans, the selective synthesis of substituted furans, specifically unsymmetrically substituted furans, is of great interest to synthetic chemists. Therefore, the development of catalytic systems capable of efficiently synthesizing substituted furans is beneficial for the continued development of medicinal and agrochemical products.

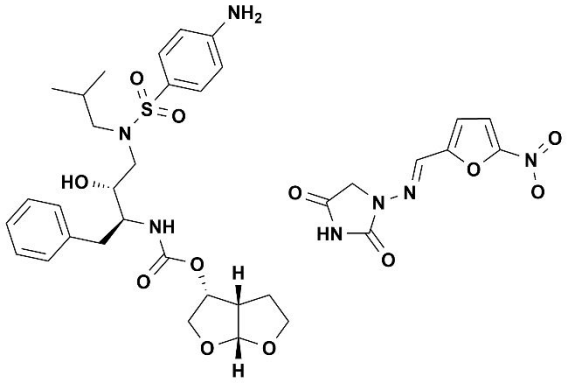

Fig 1. Structures of the HIV medication darunavir (left) and antibiotic nitrofurantoin (right).

While there are many different routes to furans, gold catalysts are commonly employed in their preparation.[18–23] Even among the gold catalysed systems, there are many different methods and catalysts for the synthesis of furans. While many studies have employed gold(III) catalysts, of particular interest for this study are gold(I) catalysts. For the intramolecular cyclization of 3-yne-1,2-diols, [Au(PPh$_3$)Cl] and silver salts were found to be efficient in catalysing the formation of furans.[24] There have been several reports finding a combination of [Au(NHC)Cl] (NHC = N-heterocyclic carbene ligands) and a silver(I) salt to be effective catalysts for the formation of furans in the reaction of 1,4-diyn-3-ols with pyridine-N-oxides.[25–28] Using similar reagents and silver salts, another study compared the efficiency of gold(I) catalysts with phosphine ligands and N-heterocyclic carbene ligands and generally found the phosphines to be the more efficient catalysts.[29] An additional study of interest to this report found [Au(NHC)Cl] to be less efficient than a dinuclear gold(I) compound with a bridging bis(NHC) ligand for the carboxylative cyclization of propargylamine.[30] These last two reports suggest that dinuclear gold(I) catalysts with bridging

701 Sullivan Road, Hugel Science Center, Department of Chemistry, Lafayette College, Easton, PA 18042, USA.
‡Current address: Department of Chemistry, Virginia Polytechnic University, Blacksburg, VA 24061, USA

c Supplementary Information (ESI) available: [
NMR spectroscopic data for [(AuCl)$_2$(dppr)] and [(AuCl)$_2$(dppo)], X-ray crystallographic details for [(AuCl)$_2$(dppr)] and [(AuCl)$_2$(dppo)], cyclic voltammograms of [(AuCl)$_2$(dppr)] and [(AuCl)$_2$(dppo)], and NMR spectroscopic data for furan products. CCDC 2117349 for [(AuCl)$_2$(dppr)] and 2117377 for [(AuCl)$_2$(dppo)]. For crystallographic data in CIF or other electronic format see . See DOI: 10.1039/x0xx00000x).

bis(phosphine)ligands could be highly efficient catalysts for furan synthesis.

Bis(phosphino)metallocene ligands are widely utilized ligands in organometallic chemistry due to their electronic and steric variability and the catalytic properties of compounds of these ligands.[31–33] The electronic and steric properties of these ligands directly influence the catalytic properties of compounds containing them and are primarily influenced by the substituents present on the phosphorous atoms. Commercially available bis(phosphino)ferrocene ligands include 1,1′-bis(diphenylphosphino)ferrocene (dppf), 1,1′-bis(ditert-butylphosphino)ferrocene (dtbpf), 1,1′-bis(diiso-propylphosphino)ferrocene (dippf), 1,1′-bis(dicyclohexylphosphino)ferrocene (dcpf), 1-(diphenylphosphino)-1′-(ditert-butylphosphino)ferrocene (dppdtbpf) and 1,1′-bis(5-methyl-2-furanylphosphino)ferrocene (dfurpf) (Table 1). In addition, the related group 8 metal variants of dppf, 1,1′-bis(diphenylphosphino)ruthenocene (dppr)[34] and 1,1′-bis(diphenylphosphino)osmocene (dppo)[35] and the related group 9 cationic ligand, 1,1′-bis(diphenylphosphino)cobaltocenium ($dppc^+$)[36] are known.

These ligands most commonly coordinate to transition metals in a bidentate manner and the majority of their activity has been examined with group 10 metals.[31–33,37,38] In recent years the study of gold catalysts containing these ligands has grown in interest due to their ability to activate unsaturated carbon-carbon bonds in cross-coupling reactions.[39] The synthesis of various gold(I) $[(AuCl)_2(\mu\text{-PP})]$ (PP = 1,1′-bis(phosphino)metallocene) compounds have been reported[39–48] and their catalytic properties have been evaluated for several organic reactions, including hydroamination and a variety of ring closing reactions.[48–51] More recently, gold catalysts have been studied in conjunction with halide abstracting agents such as $AgSbF_6$, $AgNTf_2$, and AgOTf.[52–54] In 2020, Tsurusaki examined the effectiveness of these additives in the presence of a variety of diphosphine–gold(I) complexes in an intramolecular alkyne hydroarylation of a phenol-derivative.[54] These additives were determined to be necessary for the formation of the cationic gold(I) complexes that were proposed to be the active catalysts in these reactions. High yields were achieved by pairing the diphosphine–gold(I) complexes with $AgSbF_6$ and $AgNTf_2$ additives; however, some additives resulted in low yields due to excessive amounts of silver salts present and their relative instability when coordinated with some gold(I) compounds. A comparable yield was achieved when these silver-halide abstracting agents were substituted for $Na[BArF_{24}]$ ($BArF_{24}$ = tetrakis(3,5-bis(trifluoromethyl)phenyl)borate). $Na[BArF_{24}]$ and similar halide extracting agents have grown in popularity as weakly coordinating anions that can be utilized in catalytic systems.[52] These halide abstracting agents are considered to be less coordinating, more stable and more soluble additives, capable of aiding in the formation of the cationic gold(I) species without coordinating or reacting with other reagents. In addition, utilizing halide abstraction reagents that do not contain silver eliminates the potential for silver adducts of the proposed catalyst as the reactive species, a problem noted previously.[54]

Table 1. 1,1′-Bis(phosphino)metallocene ligands

	R	R'	M	Ligand
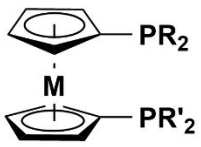	Ph	Ph	Fe	dppf
	Ph	Ph	Ru	dppr
	Ph	Ph	Os	dppo
	Ph	Ph	Co^+	$dppc^+$
	^{i}Pr	^{i}Pr	Fe	dippf
	Cy	Cy	Fe	dcpf
	^{t}Bu	^{t}Bu	Fe	dtbpf
	Ph	^{t}Bu	Fe	dppdtbpf
	5-Me-2-furanyl	5-Me-2-furanyl	Fe	dfurpf

The gold cations formed by the addition of $Na[BArF_{24}]$ to the $[(AuCl)_2(PP)]$ compounds are presumably $[Au_2(\mu\text{-Cl})(\mu\text{-PP})][BArF_{24}]$ based on the fully characterized $[Au_2(\mu\text{-Cl})(\mu\text{-dtbpf})][BArF_{20}]$ ($BArF_{20}$ = tetrakis(pentafluorophenyl)borate) formed by the reaction of $[(AuCl)_2(\mu\text{-dtbpf})]$ with $[N(p\text{-}C_6H_4Br)_3][BArF_{20}]$.[55] A variety of related gold catalysts assisted by $Na[BArF_{24}]$ have been reported in literature since. Notably, a series of $[(AuCl)_2(\mu\text{-PP})][BArF_{24}]$ compounds were reported to catalyse an intramolecular ring-closing under mild reaction conditions to produce 2,3-dimethyl furan.[35] This reaction proceeds through the gold assisted interaction of the alkyne and alcohol groups present on the starting material .[48] This study highlighted the enhanced catalytic activity $[(AuCl)_2(\mu\text{-PP})]$ compounds in the presence of $Na[BArF_{24}]$. Similarly,

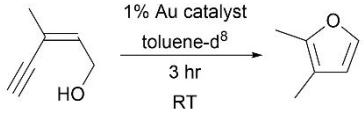

(1)

the catalytic activity of $[(AuCl)_2(\mu\text{-PP})]$ compounds in the hydroamination of phenylacetylene with various aryl amines was significantly enhanced by the addition of $Na[BArF_{24}]$.[49]

Based on these results, further exploration of the catalytic activity of these $[(AuCl)_2(\mu\text{-PP})]$ compounds with alkynes was warranted. Based on a report by Štěpnička,[56] an initial study on the reaction of phenylacetylene with pyridine-N-oxide in acetonitrile was investigated for a series of $[(AuCl)_2(\mu\text{-PP})]$ compounds in the presence of $Na[BArF_{24}]$ under similar reaction conditions to those previously reported. It was anticipated that this reaction would yield 2-methyl-5-phenyl-1,3,-oxazolne; however, the only product observed was 2,5-diphenylfuran (eqn (2)). While the gold-catalysed formation of furans from alkynes is hardly new, most of the known examples involve intramolecular ring-closing reactions.[57–62] The copper-catalysed synthesis of furans is also known[63] including a

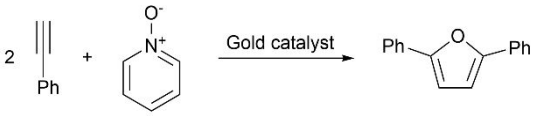

(2)

report of the [2 + 2 + 1] cycloaddition of a terminal alkyne and acetic anhydride.[64]

Herein, the gold-catalysed reaction of various terminal alkynes with the oxygen-atom donor pyridine-N-oxide to form 2,5-disubstituted furans is examined. One exception to this is the reaction of 2-pyridylethyne which yielded the unsymmetric2,4-disubstituted furan. The catalytic activity of the gold compounds showed significant dependence on the steric and electronic properties of the bis(phosphino)metallocene ligands employed in this study. In addition to the synthesis and characterization of the new compounds [$(AuCl)_2$(μ-dppr)] and [$(AuCl)_2$(μ-dppo)], the electrochemistry and X-ray crystals structures of these compounds are reported.

Results and discussion

Synthesis and characterization of [$(AuCl)_2$(dppr)] and [$(AuCl)_2$(dppo)]

Based on the synthesis of [$(AuCl)_2$([$Fe(C_5H_4P(CCPh)_2)_2$]),[65] [$(AuCl)_2$(μ-dppr)] and [$(AuCl)_2$(μ-dppo)] were prepared in good yield by the addition of a solution of [$Au(SMe_2)Cl$] to a solution of the corresponding phosphine. The compounds were characterized by NMR and like the dppf analog,[39] the signal for the phosphorous atoms of the ligands shifts downfield in the ^{31}P NMR spectrum upon coordination.

The X-ray crystal structures of [$(AuCl)_2$(μ-dppr)] and [$(AuCl)_2$(μ-dppo)] were determined (Fig. 2). The τ angle of 180°

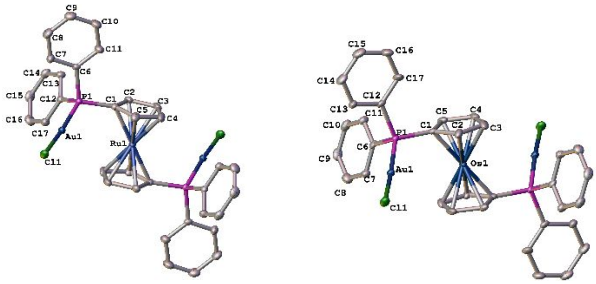

Fig 2. ORTEP drawings of [$(AuCl)_2$(μ-dppr)] (left) and [$(AuCl)_2$(μ-dppo)] (right). Ellipsoids are drawn at the 50% probability level and H atoms have been removed for clarity.

indicates that the dppr and dppo ligands adopt the antiperiplanar (staggered)[31] confirmation which is also observed in the dppf analogue (Table 2).[41] Although the intermolecular Au···Au separation is significantly shorter in the dppr and dppo compounds, these distances are still well outside of the range expected for any significant aurophilic interaction.[66] The percent buried volume ($\%V_{bur}$) is a calculated parameter based on the crystal structures related to the steric bulk of a ligand.[67] Not surprisingly, the M-X (X = centroid of the C_5 ring) distances in dppr and dppo ligands in these compounds are approximately 0.15 Å longer than that found in the dppf compound resulting in an increase of about 2% in the $\%V_{bur}$ values for dppr and dppo. While this trend was anticipated, the trend does differ from the $\%V_{bur}$ calculated for these same ligands coordinated in a bidentate mode in [$Pd(dppM)Cl_2$] (dppM = dppf, dppr or dppo). In those compounds the $\%V_{bur}$ for dppf and dppo were both calculated to be 55.5% while dppr was slightly lower at 54.7%.[68]

Table 2. Select bond lengths (Å), angles (°) and measurements for [$(AuCl)_2$(μ-dppM)] (M = Fe, Ru or Os) compounds.

	dppf[a]	dppr	dppo
Au-P	2.2282(8)	2.2198(9)	2.2206(12)
Au-Cl	2.2839(10)	2.2810(9)	2.2825(12)
M-X[b]	1.6523(13)	1.80987(11)	1.81652(4)
Au···Au	5.2695(2)	4.4730(4)	4.4776(4)
P-Au-Cl	178.51(3)	170.79(4)	170.72(5)
X-M-X[b]	180	180	180
τ[c]	180	180.0(2)	180.0(4)
θ[d]	0.0(3)	0.0 (5)	0.0 (6)
$\%V_{bur}$	33.5	35.5	35.6

[a] Reference 28.[41] [b] X is the centroid of the C_5 ring. [c] The torsion angle formed between C_a–X_a–X_b–C_b, with C being the carbon atom bonded to phosphorus. [d] The tilt angle of the C_5 rings.

The oxidative electrochemistry of [$(AuCl)_2$(μ-dppr)] and [$(AuCl)_2$(μ-dppo)] was examined using cyclic voltammetry (Table 3). Both compounds displayed a single irreversible oxidation. The oxidation of dppf displays a chemically reversible wave.[69] Upon coordination, the potential at which oxidation of the iron center of dppf occurs general shifts to more positive potentials and the wave becomes reversible as seen for [$(AuCl)_2$(μ-dppf)][47] and [$Pd(dppf)Cl_2$][69] examples. While the shift to more positive potentials upon coordination of dppr and dppo has been observed for [Pd(μ-dppr)Cl_2][69] and [Pd(-dppo)Cl_2],[70] the waves remained irreversible.

Table 3. Electrochemical data for dppM (M = Fe, Ru or Os) ligands and compounds.

	Free ligand	[$Pd(dppM)Cl_2$]	[$(AuCl)_2$(μ-dppM)]
dppf	0.24[a, b]	0.63[a, d]	0.64[d, e]
dppr	0.44[a]	0.96[a]	1.07
dppo	0.35[c]	0.85[b]	0.93

[a] Reference 56.
[b] This wave is chemically reversible.
[c] Reference 57.
[d] This wave is reversible.
[e] Reference 34.

Catalytic studies

Initial investigations into the catalytic activity of these compounds was performed with [$(AuCl)_2$(μ-dppf)] and Na[$BArF_{24}$] in acetonitrile to form oxazoles.[71,72] Unexpectedly, under these conditions the major product identified in the reaction of phenyl acetylene with pyridine-N-oxide was 2,5-diphenylfuran. The reaction conditions were optimized for the synthesis of disubstituted furans and toluene was determined to be a superior solvent to acetonitrile . Under optimized conditions, several additional systems were investigated for comparison. When the reaction was performed in the absence of both Na[$BArF_{24}$] and [$(AuCl)_2$(μ-dppf)] no product

formation was noted. When this reaction was repeated with the gold catalyst precursor ([$(AuCl)_2$(μ-dppf)]) and no Na[$BArF_{24}$],2,5-diphenylfuran formed in trace amounts. The reaction was also performed using [AuCl(PPh_3)] and Na[$BArF_{24}$], and no 2,5-diphenylfuran was detected. However, there were significant quantities of PPh_3 noted in the GC-MS trace, suggesting that the presence of the two gold centers enhances the stability of the catalyst. The catalysis was also examined using [$(AuCl)_2$(μ-dppe)] (dppe = 1,1'-bis(diphenylphosphino)ethane) which gave 2,5-diphenylfuran in 94% yield. This supports the observation that the two gold centers seem to enhance the activity of the catalyst. While efficient, the dppe catalyst was less active than three of the complexes supported by ligands with metallocene backbones. This suggests that the metallocene does enhance the catalyst activity.

Oxygen sources other than pyridine-N-oxide were screened for increased efficacy in this reaction. Replacing pyridine-N-oxide with 2-chloro-4-nitro-pyridine-N-oxide or acetophenone resulted in no product formation at the previously optimized conditions. Benzophenone was examined in place of pyridine-N-oxide and unexpectedly promoted trimerization of the alkyne yielding 1,3,5-triphenylbenzene. Further studies of this reaction are ongoing.

Similar reactions were performed using several terminal and internal alkynes (Table 4). Apart from 2-ethynylpyridine and 3,3-dimethyl-1-butyne, all terminal alkynes yielded 2,5-disubstistued furan products. Neither of the internal alkynes nor 3,3-dimethyl-1-butyne yield the corresponding furans at temperatures up to 120 °C and prolonged reaction times suggesting that steric factors can influence the efficacy of these catalysts. Even the diynes gave the [2 + 2 + 1] coupling products, 2,5-dialkynylfurans, as opposed to the intramolecular ring-closed products. In the case of 2-ethynylpyridine, furan formation still occurred, however NMR data clearly indicate that in this case the product was the 2,4-di(pyridine-2-yl)furan (eqn (3)).

Table 4. Optimized conditions for furan formation using [$(AuCl)_2$(μ-dppf)] and Na[$BarF_{24}$] in toluene.

Alkyne	Time (h)	Temp. (°C)
phenylacetylene	2	60
3-ethynyltoluene	2	60
4-tert-butylphenylacetylene	2	60
2-ethynylpyridine	4	90
1-heptyne	2	90
ethynylcyclopropane	2	90
3,3-dimethyl-1-butyne	NR	NR
3-phenyl-1-propyne	2	60
5-trimethylsilyl-4-pentyn-1-ol	NR	NR
1,6-heptadiyne	2	90
1,7-octadiyne	2	90
diphenylacetylene	NR	NR

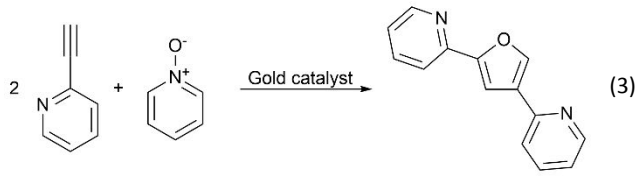

(3)

The presence of two gold centers has been noted to stabilize the catalyst in several reactions involving alkynes.[73–75] It is possible that the combination of the two gold centers and the presence of the nitrogen in the pyridyl group promotes unsymmetric substitution. The catalytic formation of an unsymmetric furan was attempted by combining equal molar amounts of phenylacetylene and 4-*tert*-butylphenylacetylene in the presence of [$(AuCl)_2$(μ-dppf)] and Na[$BArF_{24}$] but only 2,5-diphenylfuran was observed.

Upon optimizing the conditions for furan formation using [$(AuCl)_2$(μ-dppf)] and Na[$BArF_{24}$], the catalytic activity of compounds containing other bis(phosphino)metallocene ligands was examined (Table 5). Product yields were monitored using GC-MS and product identity was confirmed by NMR. While no discernible patterns emerge for the different catalysts, some generalizations can be made. Aryl substituted alkynes appear to undergo this reaction more readily than alkyl substituted alkynes. Of the substrates examined, phenylacetylene is the most likely to undergo this reaction. The steric bulk of the bis(phosphino)ferrocene ligands appears to play a significant role in the efficiency of these catalysts as the dtbpf catalyst is the worst performing catalyst in nearly every instance. Even the presence of two *tert*-butyl groups in dppdtbpf seems to have a detrimental impact on catalytic activity for most substrates. The identity of the metal in the backbone of the bis(phosphino)metallocene ligand also plays a role in the catalytic activity. As [$(AuCl)_2$(μ-dppc)]$^+$ exists as a cation prior to activation with Na[$BArF_{24}$], its solubility in toluene is limited and likely plays a role in the decreased activity of this catalyst. With respect to the group 8 metals, the activity of the catalyst decreases moving down the group. The increase in the steric bulk as indicated by the $\%V_{bur}$ could play a role in that observation as could the electron donor ability of the phosphines. A previous report found dppr to be slightly more basic than dppf[76] which would suggest that dppr is a better donor to the gold centers in the catalyst, perhaps weakening the interaction with an alkyne.

The reaction of 2-ethynylpyridine to give the 2,4-di(pyridine-2-yl)furan was the most surprising outcome of this investigation. Neither this isomer or the 3,4-di(pyridine-2-yl)furan have been reported. There have also been very few reports of the 2,5-di(pyridine-2-yl)furan. In the first report of the 2,5-isomer, it was prepared by the reaction of 1,4-di-pyridine-2-yl-1,4-butanedione with polyphosphoric acid.[77] The other reports prepared the compound from 2-ethynylpyridine[78] or 1-bromo-2-(2-ethylnylpyridine)[79] using copper(I) iodide as the catalyst. The exact role of the gold catalyst in preparing the unsymmetric2,4- isomer and the surprising efficiency of the dfurpf catalyst are unclear and warrant further investigation.

Table 5. Yields for furan forming reactions catalysed using [$(AuCl)_2$(μ-PP)] and Na[$BArF_{24}$] in toluene.

Alkyne	dppf	dppr	dppo	dppc+	dippf	dcpf	dtbpf	dppdtbpf	dfurpf
phenylacetylene	Quant.	Quant.	43%	68%	Quant.	65%	91%	83%	Quant.
3-ethynyltoluene	66%	28%	15%	8%	45%	18%	19%	8%	51%
4-*tert*-butylphenylacetylene	20%	-	-	-	12%	5%	trace	trace	15%
2-ethynylpyridine	26%	19%	17%	15%	31%	12%	-	6%	Quant.
1-heptyne	31%	10%	6%	trace	trace	5%	trace	trace	22%
ethynylcyclopropane	26%	34%	51%	20%	15%	-	trace	trace	-
3-phenyl-1-propyne	35%	29%	8%	12%	51%	60%	8%	34%	54%
1,6-heptadiyne	16%	13%	8%	trace	12%	16%	15%	24%	9%
1,7-octadiyne	42%	42%	28%	10%	47%	50%	5%	48%	45%

Experimental

General experimental methods

Preparative reactions were performed under an argon atmosphere using standard Schlenk techniques. Solvents were purchased from Fischer and used without further purification unless otherwise noted. A Solv-tek purification system was used for the purification of methylene chloride (CH_2Cl_2) and diethyl ether (Et_2O).[80] Toluene was distilled from calcium hydride under an atmosphere or argon prior to use. Tetrabutylammonium hexafluorophosphate $[NBu_4][PF_6]$, $[(AuCl)_2(dppe)]$, phenylacetylene, 4-*tert*-butylphenylacetylene and diphenylacetylene were purchased from Aldrich. The $[NBu_4][PF_6]$ was dried at 100 °C under vacuum for 24 hours prior to use. The 3-ethynyltoluene and 2-ethynylpyridine were purchased from TCI. All remaining alkyne substrates and pyridine-N-oxide were purchased from Fisher. The bis(phosphino)ferrocene ligands, ferrocene (FcH), $[AuCl(PPh_3)]$, and $[AuCl(SMe_2)]$ were purchased from Strem. The FcH was sublimed prior to use in electrochemical experiments. The $[(AuCl)_2(\mu\text{-PP})]$ (PP = dppf,[39] dippf,[44] dcpf,[45] dtbpf,[46] dppdtbpf,[47] dfurpf,[48] and (dppc+)[43]) compounds, $Na[BArF_{24}]$,[43] dppc+,[81] dppr,[34] and dppo[35] were prepared according to literature procedures. All NMR spectra were obtained in $CDCl_3$ using a Bruker Avance III HD 400 FT-NMR. The ^1H NMR and $^{13}C\{^1H\}$ spectra were referenced using internal TMS and the $^{31}P\{^1H\}$ NMR spectra were referenced using external 85% H_3PO_4. GC-MS were performed using a VG/FISONS Model MD800 Gas Chromatograph/Mass Spectrometer. Elemental analysis was performed by Midwest Microlab.

General synthetic chemical procedures

$[(AuCl)_2(\mu\text{-dppr})]$. In a flask equipped with a stir bar, $[AuCl(SMe_2)]$ (0.295 g, 1.00 mmol) was dissolved in CH_2Cl_2 (40 mL). Under a flow of argon, dppr (0.300 g, 0.500 mmol) was added. The reaction mixture was stirred for 30 min and then the volume of the solution was reduced to approximately 5 mL under vacuum. To the resulting solution, Et_2O (40 mL) was added resulting in the precipitation of a faint yellow solid. The mixture was filtered via cannula and the resulting solid was washed with Et_2O (3 x 5 mL) and dried *in vacuo*. The product was obtained as a faint yellow solid (0.396 g, 76.8 % yield). $^{31}P\{^1H\}$ NMR: δ (ppm) 28.4 (s). ^1H NMR: δ (ppm) 7.45 (m, 20H, -*Ph*), 4.98 (AA'BB', 4H, -C_5H_4), 4.63 (AA'BB', 4H, -C_5H_4). $^{13}C\{^1H\}$ NMR: δ (ppm) 133.40 (d, *J* = 13.9 Hz, DEPT +), 131.98 (d, *J* = 2.9 Hz, DEPT +), 130.18 (d, *J* = 63.1 Hz, No DEPT), 129.08 (d, *J* = 12.5 Hz, DEPT +), 78.27 (d, *J* = 8.1 Hz, DEPT +), 77.40 (d, *J* = 14.8 Hz, DEPT +) 75.55 (d, *J* = 69.7 Hz, No DEPT). Anal. Calcd for $C_{34}H_{28}Au_2Cl_2P_2Ru$: C, 38.36; H, 2.65. Found: C, 38.28; H, 2.53.

$[(AuCl)_2(\mu\text{-dppo})]$. $[AuCl(SMe_2)]$ (0.152 g, 0.517 mmol) was dissolved in CH_2Cl_2 (40 mL) in a flask equipped with a stir bar. Under a flow of argon, dppo (0.177 g, 0.260 mmol) was added. The reaction mixture was stirred for 30 min and then the volume of the solution was reduced to approximately 5 mL under vacuum. To the resulting solution, Et_2O (40 mL) was added resulting in the precipitation of a colorless solid. The mixture was filtered via cannula and the resulting solid was washed with Et_2O (3 x 5 mL) and dried *in vacuo*. The product was obtained as a colorless solid (0.188 g, 62.7 % yield). $^{31}P\{^1H\}$ NMR: δ (ppm) 31.2 (s). ^1H NMR: δ (ppm) 7.45 (m, 20H, -*Ph*), 5.17 (AA'BB', 4H, -C_5H_4), 4.79 (AA'BB', 4H, -C_5H_4). $^{13}C\{^1H\}$ NMR: δ (ppm) 133.38 (d, *J* = 13.9 Hz, DEPT +), 131.98 (br s, DEPT +), 130.17 (d, *J* = 63.8 Hz, No DEPT), 129.01 (d, *J* = 11.7 Hz, DEPT +), 72.51 (d, *J* = 8.1 Hz, DEPT +), 70.73 (d, *J* = 13.9 Hz, DEPT +), 68.80 (d, *J* = 71.9 Hz, No DEPT). Anal. Calcd for $C_{34}H_{28}Au_2Cl_2P_2Os$: C, 35.40; H, 2.45. Found: C, 35.49; H, 2.41.

X-ray data collection, solution and refinement

Crystals of $[(AuCl)_2(\mu\text{-dppr})]$ and $[(AuCl)_2(\mu\text{-dppo})]$ were grown at room temperature by vapor diffusion of Et_2O into CH_2Cl_2. Crystals were secured to a Mitegen micromount using Paratone N oil and then cooled to 100 K in a stream of N_2. Data was collected on a Rigaku XtaLAB Mini II diffractometer equipped with a Cryostream 800 cooling system and HyPix-Bantam detector. Data collection strategies ensuring completeness and desired redundancy were determined using CrysAlis^{Pro}.[82] CrysAlis^{Pro} was used for data processing and absorption corrections were applied using the SCALE3 ABSPACK scaling algorithm.[83] Using Olex2,[84] the structures were solved using ShelXT[85] and refined with ShelXL.[86] The space groups were verified via PLATON.[87] Anisotropic temperature factors were applied to all non-hydrogen atoms and hydrogen atoms were attached via the riding model.

Electrochemistry procedures

All electrochemical experiments were performed using a CH Instruments Model CHI260D potentiostat. All experiments were performed under an argon atmosphere at room temperature (22 ±

1 °C). Experiments were performed in CH_2Cl_2 (10 mL) with $[NBu_4][PF_6]$ as the supporting electrolyte. The analyte concentration was 1.0 mM and the supporting electrolyte concentration was 0.1 M. At the end of the experiment, FcH was added to the solution so the concentration of the internal standard matched that of the analyte. Background subtraction was performed for all data. Data collection occurred at intervals of 100 mV/s from 100 to 1000 mV/s using a glassy carbon working electrode (1.0 mm). Prior to use, this electrode was polished using 1.0 μm diamond paste, followed by 0.25 μm diamond paste and finally rinsed with CH_2Cl_2 prior to use. A non-aqueous Ag/AgCl electrode separated from the solution by a glass frit was used as the reference electrode and a platinum wire was used as the counter electrode.

Catalytic procedures

Catalytic reactions were performed in screw-cap glass vials with Teflon seals. A stir bar was added to the vial, followed by the addition of the desired $[(AuCl)_2(\mu\text{-PP})]$ compound (0.0125 mmol) and $Na[BArF_{24}]$ (0.0111 g, 0.0125 mmol, 1 eq.). Excess (0.0309g, 0.325 mmols) pyridine-*N*-oxide was added to the vials. The vials were then sealed and flushed with argon. Toluene (2 mL) was added and the reaction was stirred continuously. The substrates of interest were added to the solution (0.25 mmol) and the screw-cap glass vial was submerged in a heated oil bath to stir for remainder of the experiment. The optimized time and temperature was dependent on the organic reagent used (Table 2). After removing the vials from the oil bath and allowing them to cool to room temperature, 0.1 mL of solution was diluted in a GC-MS vial with 1.5 mL of toluene and 1,3,5-trimethoxybenzene (0.050 mmol) was added as an internal integration standard. Yields of the products were determined by integration of the product peak compared to 1,3,5-trimethoxybenzene. For product confirmation and characterization, a catalytic reaction mixture was passed through a column packed with silica gel using hexanes:ethyl acetate (30:1 v/v) as the eluent. The products were then confirmed by NMR.

Conclusions

During the course of this investigation, two new compounds, $[(AuCl)_2(\mu\text{-dppr})]$ and $[(AuCl)_2(\mu\text{-dppo}]$, were prepared and characterized. X-ray crystal structures of these compounds were similar to the dppf analogue, with the dppr and dppo ligands being slightly larger than the dppf ligand due to the larger 4d and 5d metal centers in the dppr and dppo ligands. The oxidative electrochemistry of these compounds exhibited a single irreversible wave, typical for compounds with dppr and dppo ligands. The potential at which oxidation of the compounds occurs follows the trend dppr > dppo > dppf which has also been observed for the free ligands and the $[Pd(PP)Cl_2]$ compounds.

Activation of the $[(AuCl)_2(\mu\text{-PP})]$ compounds by the addition of $NaBArF_{24}$ results in a catalytically active species for the formation of disubstituted furans from terminal alkynes and pyridine-N-oxide. In most cases, the product of this reaction is a 2,5-disubstituted furan with the exception of the reaction of 2-ethynylpyridine which yields the 2,4-disubstuted furan. The efficiency of the catalysis is dependent on both the nature of the terminal alkyne and the bis(phosphino)metallocene ligand. In general, the less bulky bis(phosphino)metallocene ligands give rise to more efficient catalysts. For the alkynes, phenylacetylene is the most active compound for nearly all of the catalysts examined.

Author Contributions

Reilly K. Gwinn: Investigation, Writing - original draft. Anna E. Boggess: Investigation. Elizabeth P. Winter: Investigation. Chip Nataro: Investigation, Conceptualization, Validation, Resources, Writing - review & editing, Supervision, Project administration, Funding acquisition.

Conflicts of interest

There are no conflicts to declare.

Acknowledgements

This work was partially funded by the National Science Foundation (CHE 1565648). The authors thank the Academic Research Committee at Lafayette College for their support through the EXCEL Scholars program. The authors also thank the Kresge Foundation and the McCutchen Foundation for their support in purchasing the single crystal X-ray diffractometer.

References

1 É. Lukevits and L. Demicheva, *Chemistry of Heterocyclic Compounds*, 1993, **29**, 243–267.

2 M. Alizadeh, M. Jalal, K. Hamed, A. Saber, S. Kheirouri, F. P. Fard Tabrizi and N. Kamari, *J. Inflam. Res.*, 2020, **13**, 451–463.

3 E. Loğoğlu, M. Yilmaz, H. Katircioğlu, M. Yakut and S. Mercan, *Med. Chem. Res.*, 2010, **19**, 490–497.

4 M. Koca, S. Servi, C. Kirilmis, M. Ahmedzade, C. Kazaz, B. Özbek and G. Ötük, *Eur. J. Med. Chem.*, 2005, **40**, 1351–1358.

5 C. Kirilmis, M. Ahmedzade, S. Servi, M. Koca, A. Kizirgil and C. Kazaz, *Eur. J. Med. Chem.*, 2008, **43**, 300–308.

6 G. Kirsch, A. B. Abdelwahab and P. Chaimbault, *Molecules*, 2016, **21**, 1–13.

7 K. Chand, Rajeshwari, A. Hiremathad, M. Singh, M. A. Santos and R. S. Keri, *Pharmacological Reports*, 2017, **69**, 281–295.

8 E. Boselli, K. Grob and G. Lercker, *J. Agric. Food Chem.*, 2000, **48**, 2868–2873.

9 S. S. Ghadimi, M. Alizadeh, A. T. Esfanjani, S. J. G. Hezaveh and H. J. Vayghan, *Ital. J. Food Sci.*, 2014, **26**, 169–175.

10 R. Mousavi, M. Alizadeh and S. Saleh-Ghadimi, *Eur. Food Res. Technol.*, 2016, **242**, 677–684.

11 N. Rahimzadeh, M. Alizadeh, S. Jamal and G. Hezaveh, *J. Chem. Health Risks*, 2014, **4**, 15–23.

12 K. Hannemann, V. Puchta, E. Simon, H. Ziegler, G. Ziegler and G. Spiteller, *Lipids*, 1989, **24**, 296–298.
13 D. K. Kim and J. H. Kwak, *Arch. Pharm. Res.*, 1998, **21**, 787–789.
14 G. Spiteller, *Lipids*, 2005, **40**, 755–771.
15 International Agency for Research on Cancer, *Dry Cleaning, Some Chlorinated Solvents and Other Industrial Chemicals*, 1995, vol. 63.
16 C. C. McOsker and P. M. Fitzpatrick, *J. Antimicrob. Chemotherapy*, 1994, **33A**, 23–30.
17 A. K. Ghosh, Z. L. Dawson and H. Mitsuya, *Bioorg. Med. Chem.*, 2007, **15**, 7576–7580.
18 A. Blanc, V. Beneteau, J.-M. Weibel and P. Pale, *Org. Biomol. Chem.*, 2016, **14**, 9184–9205.
19 A. Deepthi, B. P. Babu and A. L. Balachandran, *Org. Prep. Proc. Int.*, 2019, 51, 409–442.
20 D. X. Duc, *Mini-Rev. Org. Chem.*, 2018, **16**, 422–452.
21 F. Gao, Y. Zhou and H. Liu, *Curr. Org. Chem.*, 2017, **21**, 1530-1566.
22 D. Pflästerer and A. S. K. Hashmi, *Chem. Soc. Rev.*, 2016, **45**, 1331–1367.
23 L. P. Liu and G. B. Hammond, *Chem. Soc. Rev.*, 2012, **41**, 3129–3139.
24 M. Egi, K. Azechi and S. Akai, *Org. Lett.*, 2009, **11**, 5002–5005.
25 T. Wang, S. Shi, M. Rudolph and A. S. K. Hashmi, *Adv. Synth. Catal.*, 2014, **356**, 2337–2342.
26 T. Wang, L. Huang, S. Shi, M. Rudolph and A. S. K. Hashmi, *Chem. Eur. J.*, 2014, **20**, 14868–14871.
27 T. Wang, S. Shi, M. M. Hansmann, E. Rettenmeier, M. Rudolph and A. S. K. Hashmi, *Angew. Chem., Int. Ed.*, 2014, **53**, 3715–3719.
28 X. Xiao, S. Liu and M. Cai, *J. Organomet. Chem.*, 2022, 122527.
29 N. Rode, F. Marinelli, A. Arcadi, T. Adak, M. Rudolph, F. Rominger and A. S. K. Hashmi, *Adv. Synth. Catal.*, 2018, **360**, 4790–4794.
30 T. A. C. A. Bayrakdar, F. Nahra, J. v. Davis, M. M. Gamage, B. Captain, M. Temprado, M. Marazzi, M. Saab, K. van Hecke, D. Ormerod, C. D. Hoff and S. P. Nolan, *Organometallics*, 2020, **39**, 2907–2916.
31 K.-S. Gan and T. S. A. Hor, in *Ferrocenes: Homogeneous catalysis, organic synthesis, materials science*, eds. A. Togni and T. Hayashi, VCH, Weinheim, Germany, 1995, pp. 3–104.
32 S. W. Chien and T. S. A. Hor, in *Ferrocenes: Ligands, materials and biomolecules*, ed. P. Štěpnička, John Wiley & Sons, Inc., West Sussex, England, 2008, pp. 33–116.
33 T. J. Colacot and S. Parisel, in *Ferrocenes: Ligands, materials and biomolecules*, ed. P. Štěpnička, John Wiley & Sons, Inc., West Sussex, England, 2008, pp. 117–140.
34 S. Li, B. Wei, P. M. N. Low, H. K. Lee, T. S. A. Hor, F. Xue and T. C. W. Mak, *J. Chem. Soc., Dalton Trans.*, 1997, 1289–1293.
35 O. V. Gusev, A. M. Kalsin, P. V. Petrovskii, K. A. Lyssenko, Y. F. Oprunenko, C. Bianchini, A. Meli and W. Oberhauser, *Organometallics*, 2003, **22**, 913–915.
36 C. C. Brasse, U. Englert, A. Salzer, H. Waffenschmidt and P. Wasserscheid, *Organometallics*, 2000, **19**, 3818–3823.
37 P. Štěpnička, in *Ferrocenes: Ligands, materials and biomolecules*, ed. P. Štěpnička, John Wiley & Sons, Inc., West Sussex, England, 2008, pp. 177–204.
38 H.-U. Blaser, W. Chen, F. Camponovo and A. Togni, in *Ferrocenes: Ligands, materials and biomolecules*, ed. P. Štěpnička, John Wiley & Sons, Inc., West Sussex, England, 2008, pp. 205–236.
39 D. T. Hill, G. R. Girard, F. L. McCabe, R. K. Johnson, P. D. Stupik, J. H. Zhang, W. M. Reiff and D. S. Eggleston, *Inorg. Chem.*, 1989, **28**, 3529–3533.
40 O. Crespo, M. C. Gimeno, P. G. Jones and A. Laguna, *Acta Crystallogr., Sect. C: Cryst. Struct. Commun.*, 2000, **C56**, 1433–1434.
41 E. C. Constable, C. E. Housecroft, M. Neuburger, S. Schaffner and E. Shardlow, *Acta Crystallogr., Sect. E: Struct. Rep. Online*, 2007, **E63**, m1697.
42 N. Meyer, F. Mohr and E. R. T. Tiekink, *Acta Crystallogr., Sect. E: Struct. Rep. Online*, 2010, **E66**, m168–m169.
43 Y. Chen, X.-H. Wu, G.-A. Yu, S. Jin, X.-G. Meng and S.-H. Liu, *Transition Met. Chem.*, 2009, **34**, 103–108.
44 J. H. L. Ong, C. Nataro, J. A. Golen and A. L. Rheingold, *Organometallics*, 2003, **22**, 5027–5032.
45 L. E. Hagopian, A. N. Campbell, J. A. Golen, A. L. Rheingold and C. Nataro, *J. Organomet. Chem.*, 2006, **691**, 4890–4900.
46 F. N. Blanco, L. E. Hagopian, W. R. McNamara, J. A. Golen, A. L. Rheingold and C. Nataro, *Organometallics*, 2006, **25**, 4292–4300.
47 S. L. Kahn, M. K. Breheney, S. L. Martinak, S. M. Fosbenner, A. R. Seibert, W. S. Kassel, W. G. Dougherty and C. Nataro, *Organometallics*, 2009, **28**, 2119–2126.
48 T. A. Michaels, O. F. Pritchard, J. S. Dell, M. W. Bezpalko, W. S. Kassel and C. Nataro, *J. Organomet. Chem.*, 2019, **889**, 1–8.
49 S. A. Wolfarth, N. E. Miner, N. E. Wamser, R. K. Gwinn, B. C. Chan and C. Nataro, *J. Organomet. Chem.*, 2020, **906**, 121049.
50 S. Ibáñez, M. Poyatos, L. N. Dawe, D. Gusev and E. Peris, *Organometallics*, 2016, **35**, 2747–2758.
51 T. V. Segapelo, I. A. Guzei and J. Darkwa, *J. Organomet. Chem.*, 2008, **693**, 701–708.
52 Y. He, Z. Li, K. Robeyns, L. Van Meervelt and E. V. Van der Eycken, *Angew. Chem., Int. Ed.*, 2018, **57**, 272–276.
53 C. Chen and S. Cui, *J. Org. Chem.*, 2019, **84**, 12157–12164.
54 A. Tsurusaki, R. Ura and K. Kamikawa, *Organometallics*, 2020, **39**, 87–92.
55 S. F. Hartlaub, N. K. Lauricella, C. N. Ryczek, A. G. Furneaux, J. D. Melton, N. A. Piro, W. S. Kassel and C. Nataro, *Eur. J. Inorg. Chem.*, 2017, **2017**, 424–432.
56 K. Škoch, I. Císařová and P. Štěpnička, *Chem. Eur. J.*, 2015, **21**, 15998–16004.
57 A. S. K. Hashmi, *Chem. Rev.*, 2007, **107**, 3108–3211.
58 X. Du, F. Song, Y. Lu, H. Chen and Y. Liu, *Tetrahedron*, 2009, **65**, 1839–1845.
59 Y. Wang and L. Zhang, *Synthesis*, 2015, **47**, 289–305.

60 Z. Zheng, Z. Wang, Y. Wang and L. Zhang, *Chem. Soc. Rev.*, 2016, **45**, 4448–4458.
61 N. Kaur, *Inorg. Nano-Met. Chem.*, 2017, **47**, 163–187.
62 S. A. Shahzada, M. A. Sajid, Z. A. Khan and D. Canseco-Gonzalezb, *Synth. Commun.*, 2017, **47**, 735–755.
63 T. Pal, G. K. Lahiri and D. Maiti, *Eur. J. Org. Chem.*, 2020, **2020**, 6859–6869.
64 H. Lee, Y. Yi and C. H. Jun, *Adv. Synth. Catal.*, 2015, **357**, 3485–3490.
65 P. Sameer Prasad, M. K. Pandey and M. S. Balakrishna, *Polyhedron*, 2019, **158**, 173–182.
66 H. Schmidbaur and A. Schier, *Chem. Soc. Rev.*, 2012, **41**, 370–412.
67 L. Falivene, Z. Cao, A. Petta, L. Serra, A. Poater, R. Oliva, V. Scarano and L. Cavallo, *Nat. Chem.*, 2019, **11**, 872–879.
68 H. Clavier and S. P. Nolan, *Chem. Commun.*, 2010, **46**, 841–861.
69 C. Nataro, A. N. Campbell, M. A. Ferguson, C. D. Incarvito and A. L. Rheingold, *J. Organomet. Chem.*, 2003, **673**, 47–55.
70 S. L. Martinak, L. A. Sites, S. J. Kolb, K. M. Bocage, W. R. McNamara, A. L. Rheingold, J. A. Golen and C. Nataro, *J. Organomet. Chem.*, 2006, **691**, 3627–3632.
71 W. He, C. Li and L. Zhang, *J. Am. Chem. Soc.*, 2011, **133**, 8482–8485.
72 Q. Wang, S. Hoffmann, J. Schießl, M. Rudolph, F. Rominger and A. S. K. Hashmi, *Eur. J. Org. Chem.*, 2020, **2020**, 2384–2388.
73 R. Uson, A. Laguna and M. V. Castrillo, *Synth. React. Inorg. Met.-Org. Chem.*, 1979, **9**, 317–324.
74 A. Bayler, A. Bauer and H. Schmidbaur, *Chem. Ber./Recueil*, 1997, **130**, 115–118.
75 A. S. K. Hashmi, M. C. Blanco, E. Kurpejović, W. Frey and J. W. Bats, *Adv. Synth. Catal.*, 2006, **348**, 709–713.
76 A. R. O'Connor and C. Nataro, *Organometallics*, 2004, **23**, 615–618.
77 R. A. Jones and P. U. Civcir, *Tetrahedron*, 1997, **53**, 11529–11540.
78 Y. Li, L. Cheng, L. Chen, B. Li, N. Sun and N. Qing, *Chinese J. Org. Chem.*, 2016, **36**, 2426–2436.
79 H. Jiang, W. Zeng, Y. Li, W. Wu, L. Huang and W. Fu, *J. Org. Chem.*, 2012, **77**, 5179–5183.
80 A. B. Pangborn, M. A. Giardello, R. H. Grubbs, R. K. Rosen and F. J. Timmers, *Organometallics*, 1996, **15**, 1518–1520.
81 J. Guan, G.-A. Yu, J.-G. Hou, N. Yu, Y. Ren and S. H. Liu, *Appl. Organomet. Chem.*, 2007, **21**, 355–359.
82 CrysAlisPro 1.171.41.118a (Rigaku Oxford Diffraction, 2021).
83 R. C. Clark and J. S. Reid, *Acta Cryst.*, 1995, **A51**, 887-897.
84 O. V. Dolomanov, L. J. Bourhis, R. J. Gildea, J. A. K. Howard and H. Puschmann, *J. Appl. Cryst.*, 2009, **42**, 339–341.
85 G. M. Sheldrick, *Acta Crystallogr., Sect. A: Found. Adv.*, 2015, **71**, 3–8.
86 G. M. Sheldrick, *Acta Crystallogr., Sect. C: Cryst. Struct. Commun.*, 2015, **71**, 3–8.
87 A. L. Spek, *Acta Crystallogr., Sect. D: Biol. Cryst.*, 2009, **65**, 148–155.